

## Quantum scattering of neon from a nanotextured surface

This article has been downloaded from IOPscience. Please scroll down to see the full text article.

2009 J. Phys.: Condens. Matter 21 225009

(<http://iopscience.iop.org/0953-8984/21/22/225009>)

View [the table of contents for this issue](#), or go to the [journal homepage](#) for more

Download details:

IP Address: 129.252.86.83

The article was downloaded on 29/05/2010 at 20:05

Please note that [terms and conditions apply](#).

# Quantum scattering of neon from a nanotextured surface

A C Levi<sup>1</sup>, C Huang<sup>2,4</sup>, W Allison<sup>2</sup> and D A MacLaren<sup>2,3</sup>

<sup>1</sup> Dipartimento di Fisica and CNISM, Università di Genova, 16146 Genova, Italy

<sup>2</sup> Cavendish Laboratory, University of Cambridge, J J Thomson Avenue, Cambridge CB3 0HE, UK

<sup>3</sup> Department of Physics and Astronomy, University of Glasgow, Glasgow G12 8QQ, UK

E-mail: [levi@fisica.unige.it](mailto:levi@fisica.unige.it) and [dmaclaren@physics.org](mailto:dmaclaren@physics.org)

Received 9 February 2009, in final form 16 April 2009

Published 11 May 2009

Online at [stacks.iop.org/JPhysCM/21/225009](http://stacks.iop.org/JPhysCM/21/225009)

## Abstract

Phonon exchange is the usual cause of decoherence in atom–surface scattering. By including quantum effects in the treatment of Debye–Waller scattering, we show that phonon exchange becomes ineffective when the relevant phonon frequencies are high. The result explains the surprising observation of strong elastic scattering of Ne from a Cu(100) surface nanotextured with a  $c(2 \times 2)$  Li adsorbate structure. We extend a previous model to describe the phonon spectra by an Einstein oscillator component with an admixture of a Debye spectrum. The Einstein oscillator represents the dominant, high frequency vibration of the adsorbate, normal to the surface, while the Debye spectrum represents the substrate contribution. Neon scattering is so slow that exciting the adsorbate mode has a low probability and is impossible if the incident energy is below the threshold. Thus, adsorbate vibrations are averaged out. A theoretical discussion and calculation shows that under such circumstances the vibrations of a light adsorbate do not contribute to the Debye–Waller effect, with the result that Ne scattering at thermal energies is quantum mechanical and largely elastic, explaining the high reflectivity and the diffraction peaks observed experimentally.

(Some figures in this article are in colour only in the electronic version)

## 1. Introduction

Rare gas atoms are ideal probes of surfaces and ideal prototypes for understanding fundamental aspects of atom–surface interactions. If the surface exhibits a well-ordered, two-dimensional crystal lattice, then diffraction—a typical quantum effect—may occur and afford detailed information on surface crystallography. However, diffraction is usually strong only for thermal energy helium, due to its small mass. Inelastic scattering tends to dominate for heavier probe atoms unless particular experimental conditions, such as low surface temperatures or grazing incidence reflection, are adopted [1–14]. Unexpectedly, early neon atom scattering measurements also revealed diffraction peaks [1, 2], even though the ordinary Debye–Waller theory predicted them to be unobservably weak. An extension of that theory was

soon presented [15] (and has since been refined [16–19]<sup>5</sup>) and explained the result by showing that the time decay of the displacement correlation functions causes a decrease of the effective disorder seen during scattering. Diffraction was therefore observed simply because thermal energy neon is relatively slow and the scattering interaction is correspondingly long. Neon scattering from surfaces has since been studied by several other groups [3–7, 20], although generally only for surfaces with simple, fixed properties. Much of the recent theoretical work has concentrated on either the nature of the adiabatic potential (see, for example [21, 22]), or in describing the scattering from a classical perspective [13, 23]. Recently, we described the first experiments of neon scattering from a metallic thin film [24], where the properties of the

<sup>4</sup> Present address: Stanford Linear Accelerator Center, 2575 Sand Hill Road, Menlo Park, CA94025, USA.

<sup>5</sup> We make no use of these theoretical advances here because, on one hand [16] refers to the different situation of very low temperatures (in particular,  $T = 0$ ), and on the other, the more refined theory of [17–19] is fully quantal but only differs substantially from the semiclassical theory of [15] for very small masses such as He or H<sub>2</sub> [7].

surface vary strongly with the atom density in the film. Intriguingly, we demonstrated that changes to surface *structure* can also enhance quantum scattering, leading to the unexpected result that even a room temperature neon beam can diffract strongly from an overlayer of lithium with little inelastic losses. The result is counter-intuitive since standard Debye–Waller scattering models predict that, in comparison with helium–surface scattering, increasing the probe particle mass and decreasing the effective surface mass should enhance inelastic events and thereby strongly attenuate the diffractive intensity.

In the present paper we aim to provide a qualitative explanation for the quantum scattering of Ne, the experimental evidence for which is summarized in section 2. We recap the basic Debye–Waller theory appropriate to atom scattering [15] in section 3. In section 4 the theory is then extended to consider quantum corrections and the particular case of an Einstein model of adsorbate phonons, including the possibility of there being more than one contribution to the phonon spectrum. This section expands upon a qualitative model that was previously only outlined [24]. In section 5 we compare our results with the experimental data. Our main point is to show that phonon exchange, which usually causes decoherence in atom–surface scattering, can become ineffective when the only accessible phonons have high frequencies. In that case, the scattered atoms are hardly able to excite or absorb surface phonons, and therefore remain coherent, resulting in high reflectivity and the appearance of diffraction peaks.

## 2. Scattering experiments on adsorbate-covered copper

The experiment was conducted as outlined in [24] and the key data are reproduced in figure 1, which compares the variations in He and Ne reflectivity of Li/Cu(100) during submonolayer lithium deposition. The clean Cu(100) substrate, at 0 monolayers (ML) in the figure, showed a characteristic strong He reflectivity, whilst Ne reflectivity was attenuated by the usual Debye–Waller scattering, giving a ratio of He reflectivity to Ne reflectivity of around 5:1—i.e. in broad agreement with existing theory [15] and the mass-difference between He and Ne. As lithium was deposited onto the Cu(100) surface, the He and Ne reflectivities behave similarly except for a striking, five-fold increase in Ne reflectivity approaching a coverage of 0.5 ML, where a  $c(2 \times 2)$ Li/Cu(100) overlayer forms. Remarkably, the He and Ne reflectivities are almost identical for this overlayer structure, and the ratio of reflectivities is measured to be 1.0. Further investigation revealed that the dramatic increase in Ne specular reflectivity is due to a near-total extinction of inelastic scattering [24, 25]. Thus, the loss of a broad angular distribution of inelastic-scattered Ne gives a concomitant increase in elastic scattering in the specular direction. The observed changes in the peak profile, and the emergence of clear diffraction peaks [24], indicate that the effect cannot be described within a conventional classical analysis [23]. At higher surface coverages, reflectivity again reduces and a broad, diffuse scattered Ne signal indicates the return of multiphonon effects. Thus, the increased quantum character

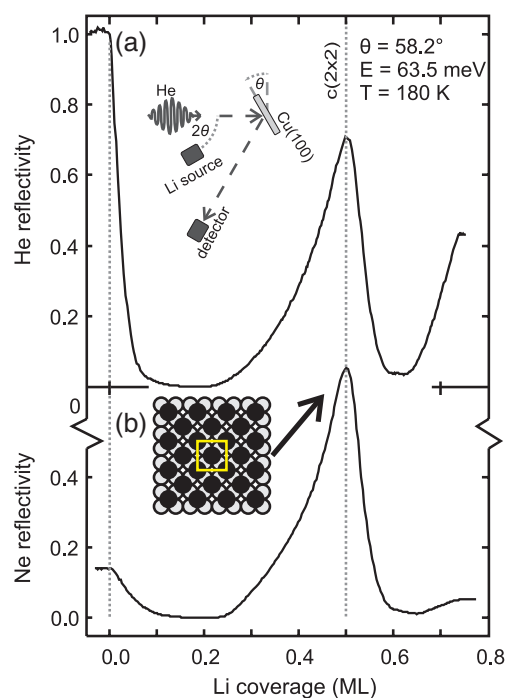


**Figure 1.** The variation of (a) He and (b) Ne reflectivity of a Cu(100) substrate during submonolayer Li deposition. The scattering geometry is indicated in the inset to (a) and a cartoon of the  $c(2 \times 2)$ Li/Cu(100) structure (unit cell indicated), which is formed at a coverage of 0.5 ML, is inset in (b). The data are normalized to allow direct comparison between the two traces and with respect to the background-subtracted He reflectivity of the Cu(100) substrate. Simplistically, reductions in specular intensity are caused by diffuse scattering from disordered Li adatoms whilst increases in reflectivity indicate an increase in surface ordering. He and Ne have similar reflectivities between 0.3 and 0.6 ML, suggesting a lack of inelastic Ne scattering in this regime. See [24] for more details.

and reduced energy exchange is strongly dependent not only on the chemical identity, but also on the geometric structure of the overlayer.

Only the  $c(2 \times 2)$ Li/Cu(100) structure is relevant here and, as outlined below, can be associated with a significant reduction of the Debye–Waller exponent,  $W$ , for Ne. Does this mean that Ne is as quantum mechanical as He, or even more? Of course not. As will be shown, the effect is a consequence of the heavier Ne atom taking much longer to cross the atom-metal potential. In this way, the effects of atomic vibrations are averaged out and everything happens as if the alkali atoms were immobile at their equilibrium positions. As a result, multiphonon effects are quenched and the effective Debye–Waller exponent is small.

## 3. Debye–Waller factor in atom–surface scattering

In order to explain the experimental results, we begin by recapping the model of Debye–Waller attenuation that has become routine in the theoretical treatment of atom–surface scattering. In quantum scattering theory the relevant information is contained in the  $T$ -matrix, which here is to be evaluated between states compounded of a particle state,

labelled by a wavevector  $\mathbf{k}$ , and a crystal state  $|u\rangle$  (where  $u$  is shorthand for a certain set of phonon occupation numbers). It is convenient to write the initial ( $\mathbf{k}_i$ ) and final ( $\mathbf{k}$ ) wavevectors as subscripts, in such a way that a  $\mathbf{T}$ -matrix element is written as  $\langle v|T_{\mathbf{k}\leftarrow\mathbf{k}_i}|u\rangle$  and  $T_{\mathbf{k}\leftarrow\mathbf{k}_i}$  can be considered as an operator on the space of crystal states. The differential probability that an atom scatters into the solid angle  $d\Omega$ , losing the positive (or negative) amount of energy  $\Delta$  to the crystal, is given by

$$dP = \frac{L^4 m^2 |\mathbf{k}|}{4\pi^2 \hbar^4 |\mathbf{k}_{iz}|} \sum_u P_u \sum_v |\langle v|T_{\mathbf{k}\leftarrow\mathbf{k}_i}|u\rangle|^2 \times \delta(E_v - E_u - \Delta) d\Omega d\Delta. \quad (1)$$

Here,  $m$  is the atom mass;  $L$  is an appropriate quantization length;  $E_u$  and  $E_v$  are the crystal energies before and after scattering, respectively;  $P_u$  is the probability of the crystal phonon system to be in state  $u$ ; and the prefactor has been written in a form appropriate to scattering from surfaces. Under the strong scattering conditions of atom scattering, the van Hove transformation (originally introduced for the weak scattering conditions of neutron scattering [26]) can still be applied, except that the full  $\mathbf{T}$ -matrix must be kept, obtaining

$$dP = \frac{L^4 m^2 |\mathbf{k}|}{8\pi^3 \hbar^5 |\mathbf{k}_{iz}|} d\Omega d\Delta \times \int \exp\left(-\frac{it\Delta}{\hbar}\right) \langle T_{\mathbf{k}\leftarrow\mathbf{k}_i}^\dagger(0) T_{\mathbf{k}\leftarrow\mathbf{k}_i}(t) \rangle dt. \quad (2)$$

Note that for the correlation occurring in (2) the momenta must be specified; moreover  $\mathbf{T}$  is not self-adjoint, although the atom-crystal scattering potential  $\mathbf{V}$  may be treated as such.

The Fourier transforms occurring in (2) are not well behaved because the correlation functions do not vanish when  $t \rightarrow \infty$ . For long times (where the  $\mathbf{T}$ -matrices become uncorrelated) the limit is  $|\langle T_{\mathbf{k}\leftarrow\mathbf{k}_i} \rangle|^2$  and gives rise to *elastic scattering*, hence to all diffraction effects, while the remainder gives rise to inelastic scattering. Focusing on the former, the probability of an atom scattering elastically into the solid angle  $d\Omega$  is then

$$dP_{\text{elastic}} = \frac{L^4 m^2}{4\pi^2 \hbar^4 \cos \theta_i} |\langle T_{\mathbf{k}\leftarrow\mathbf{k}_i} \rangle|^2 d\Omega. \quad (3)$$

Both (2) and (3) are exact, but approximations are required to use them in practice and the simple, semiclassical eikonal approximation [11, 15, 27] will be used here:

$$T_{\mathbf{k}\leftarrow\mathbf{k}_i} = -i \frac{\hbar^2 |\mathbf{k}_{iz}|}{mL^3} \int \exp[i\eta(\mathbf{R}, t)] d^2R, \quad (4)$$

where the phase,  $\eta$ , equals the action,  $\mathcal{S}$ , divided by  $\hbar$ , and the diffraction integral over the surface is a reminder of the enormously more complex Feynman path integral that would appear in an exact formulation. The phase  $\eta$  can be split into a time-independent, perfect crystal contribution  $\eta^{(0)} = \mathbf{Q} \cdot \mathbf{R} + \eta'$  (where  $\hbar\mathbf{Q}$  is the momentum transfer parallel to the surface and  $\eta'$  is periodic in  $\mathbf{R}$ ) and a contribution  $\delta\eta(\mathbf{R}, t)$  from the crystal vibrations, which is linear in the displacements. It is the latter that is especially interesting for energy exchange. Because of the mean,  $\langle T \rangle$ , occurring in (3), the average

$$\langle \exp[i\delta\eta(\mathbf{R}, t)] \rangle = \exp[-W(\mathbf{R})] \quad (5)$$

must be considered, where  $W(\mathbf{R}) = \frac{1}{2} \langle [\delta\eta(\mathbf{R})]^2 \rangle$ . Equation (5) already has a Debye–Waller form, but is still  $\mathbf{R}$ -dependent. However, for each individual diffraction peak (corresponding to the reciprocal lattice vector  $\mathbf{G}$ ), most of the contribution to the integral comes from those regions of the surface from which scattering occurs with the momentum transfer  $\hbar\mathbf{Q} = \hbar\mathbf{G}$ . Then  $W$  is effectively to be computed there, obtaining  $W_{\mathbf{G}}$  and a constant exponential factor  $\exp(-W_{\mathbf{G}})$  that may be extracted from the integral. Since  $\langle T \rangle$  appears squared in (3), the *Debye–Waller factor*

$$e^{-2W_{\mathbf{G}}} \quad (6)$$

is obtained. This is the only effect of the crystal vibrations on the probability of the  $\mathbf{G}$ -diffraction.

Now,  $\delta\eta = \delta\mathcal{S}/\hbar$  and  $\delta\mathcal{S}$ , the action fluctuation, equals (minus) the integral over time of the work fluctuation, i.e. the sum over the crystal ions of the scalar product of the force  $\mathbf{F}_n$  operated by the atom on the  $n$ -th ion times the ion displacement  $\mathbf{u}_n$ :

$$\delta\mathcal{S} = - \sum_n \int \mathbf{F}_n(t) \cdot \mathbf{u}_n(t) dt. \quad (7)$$

Thus,  $W_{\mathbf{G}}$  is written as the integral over collision times  $\tau = t' - t$  of a product of (tensorial) correlations, with a double sum over the ions, giving the main result of [15]:

$$W_{\mathbf{G}} = \frac{1}{2\hbar^2} \sum_{mn} \int A_{mn}(\tau) : B_{mn}(\tau) d\tau \quad (8)$$

where the tensors  $A$  and  $B$  are given by

$$A_{mn}(\tau) = \int \mathbf{F}_m(t) \mathbf{F}_n(t + \tau) dt \quad (9)$$

and

$$B_{mn}(\tau) = \langle \mathbf{u}_m(0) \mathbf{u}_n(\tau) \rangle. \quad (10)$$

Let us now simplify the above result to consider the interaction with only one crystal atom at a time and to assume the same Debye–Waller factor for all diffraction peaks. These simplifications allow us to consider the dominant term in the inelastic atom–surface interaction and, in simple cases, provide a good description of rare gas scattering [11]. The approximation is particularly appropriate for the Einstein model developed below, since Einstein oscillators are independent and thus collisions with multiple adsorbates account for relatively small contributions. The Debye–Waller exponent is now obtained by replacing (8) with the far simpler formula

$$W = \frac{1}{2\hbar^2} \int A(\tau) B(\tau) d\tau, \quad (11)$$

where, again,  $A(\tau)$  refers to the correlation of scattering forces and  $B(\tau)$  to the correlations of crystal vibrations but where the summation over the entire lattice,  $(m, n)$ , has been dropped. The latter term has been calculated previously for a Bravais lattice of atoms of mass  $M$  vibrating perpendicularly with a vibrational spectrum  $g(\omega)$  [15, 28] and yields

$$B(\tau) = \frac{\hbar}{M} \int \frac{g(\omega)}{\omega} \left( \frac{\cos(\omega\tau)}{e^{\hbar\omega/kT} - 1} + \frac{1}{2} e^{i\omega\tau} \right) d\omega. \quad (12)$$

Here,  $k$  is Boltzmann's constant. Classically (i.e. at temperatures so high that the zero-point vibrations may be neglected) this may be simplified to

$$B(\tau) = \frac{kT}{M} \int \frac{g(\omega)}{\omega^2} \cos(\omega\tau) d\omega. \quad (13)$$

Even the force correlation  $A(\tau)$  can be evaluated explicitly, by assuming that the atom–surface potential is a Morse potential. One ends up with:

$$W = \frac{2\pi^2 m^2 kT}{\hbar^2 M \alpha^2} \int \frac{\cosh^2(\pi\beta\omega\tau_c)}{\sinh^2(\pi\omega\tau_c)} g(\omega) d(\omega), \quad (14)$$

where  $m$  is the mass of the incident particle and  $\alpha$  is the Morse potential parameter, giving a collision time,  $\tau_c = 1/(\alpha v_z)$ , with an initial perpendicular velocity  $v_z$ . The arguments of the hyperbolic cosine and sine differ only by a factor

$$\beta = 1 - \frac{1}{\pi} \tan^{-1} \sqrt{\frac{E_z}{\varepsilon}}, \quad (15)$$

for an initial perpendicular kinetic energy  $E_z$  and potential well of depth  $\varepsilon$  [15].

For a fast projectile,  $\omega\tau_c$  would be small for most of the phonon spectrum. Then the approximations  $\cosh^2(\pi\beta\omega\tau_c) \approx 1$  and  $\sinh^2(\pi\omega\tau_c) \approx \pi^2\omega^2\tau_c^2$  would apply, leading to the conventional expression

$$W = \Omega^2 \int \frac{g(\omega)}{\omega^2} d\omega, \quad (16)$$

where  $\Omega = q(kT/2M)^{1/2}$ , for momentum transfer  $q$ : i.e. to the elementary Debye–Waller theory. For Ne scattering, however,  $\omega\tau_c$  is relatively large and (14) rather than (16) should be expanded for the appropriate phonon density of states. For example, consider a Debye spectrum with characteristic Debye angular frequency  $\omega_D$ , leading to Debye–Waller exponent,  $W_D$ . Then  $g(\omega) = 3\omega^2/\omega_D^3$  for  $\omega < \omega_D$  (and zero otherwise), giving

$$W_D = \frac{12mE_z kT}{\hbar^2 M \omega_D^2} S \quad (17)$$

with

$$S = \frac{1}{\pi\omega_D\tau_c} \int_0^{\pi\omega_D\tau_c} \frac{\cosh^2(\beta x)}{\sinh^2(x)} x^2 dx, \quad (18)$$

which is the result of the elementary theory modified by a ‘slow correction term’,  $S$ . Analysis of  $S$  is provided in [15]: for small values of  $\pi\omega_D\tau_c$ , it is shown that  $S \approx 1$ , whilst for large values of  $\pi\omega_D\tau_c$  and shallow potential wells,  $S \approx 2/(\pi\omega_D\tau_c)$ , giving substantial enhancement of reflectivity.

#### 4. Scattering from an Einstein model

Let us now consider the data of figure 1 and the scattering of thermal energy Ne from  $c(2 \times 2)\text{Li}/\text{Cu}(100)$ . We will use an Einstein model, an approximation that will only describe the dominant effect but is validated by its ability to describe the experimental data rather well and its successful application to a number of related systems with dispersionless modes [29–32].

We therefore model  $c(2 \times 2)\text{Li}/\text{Cu}(100)$  as an overlayer of independent oscillators with a phonon spectrum defined by the purely perpendicular vibrations of adsorbed atoms, all with a frequency  $\omega_E$ . A very different frequency spectrum refers to any parallel motions; however, He scattering measurements on the related  $c(2 \times 2)\text{Na}/\text{Cu}(100)$  system show an extinction of coupling to low-energy T-mode (parallel to surface) phonons for the  $c(2 \times 2)$  structure [33], so we later consider any residual coupling to T-modes as a relatively small correction to the Einstein model. For the moment, let us consider only the perpendicular oscillations. The spectrum, rather trivially, is a  $\delta$ -function:

$$g(\omega) = C_E \delta(\omega - \omega_E) \quad (19)$$

where the prefactor,  $C_E$ , gives a weighting that we set to one at present and which will be considered in more detail below. Using (14), the Debye–Waller exponent for the Einstein oscillator,  $W_E$ , becomes

$$W_E = Q \frac{2\pi^2 m^2 kT}{\hbar^2 M \alpha^2} \frac{\cosh^2(\pi\beta\omega_E\tau_c)}{\sinh^2(\pi\omega_E\tau_c)}. \quad (20)$$

Here, we have also introduced a quantum correction factor,  $Q(\frac{\hbar\omega}{kT}, \frac{\hbar\omega}{E_z})$ , which will be discussed in detail shortly. We note two interesting consequences of (20) at this stage. First, there is an explicit dependence on the terms  $\alpha$ , which defines the range of the Morse potential, and  $\beta$ , which is determined by the incident energy in relation to the depth of the well in the Morse potential. Second, the variation of  $W_E$  as a function of the mass of the incident particle differs from that of either the conventional Debye–Waller exponent, (16), or that for slow atoms scattering classically from a surface with a Debye vibrational spectrum, (17). The new mass dependence follows from (20), noting that  $\beta$  is less than 1, and that, for a given incident energy,  $\tau_c$  is proportional to  $\sqrt{m}$ . Thus, for small masses the ratio of the hyperbolic functions simplifies to

$$\frac{2\alpha^2 E_z}{\pi^2 m \omega_E^2}, \quad (21)$$

and so is proportional to  $m^{-1}$ . Meanwhile, the first term in (20) is proportional to  $m^2$ , ignoring for the present any mass dependence in  $Q$ . It therefore follows that the Debye–Waller exponent for scattering from an Einstein oscillator,  $W_E$ , is proportional to  $m$  in the limit of small mass. For large masses, however, the ratio of the hyperbolic functions decreases exponentially, so  $W_E$  rises to a maximum before decreasing as mass increases further. This mass dependence is much stronger than the corresponding behaviour for a Debye spectrum (17), where the  $m$  dependence (by virtue of  $\tau_c$ ) of the slow correction term,  $S$ , gives a  $\sqrt{m}$  dependence of  $W_D$  at low energies. The weaker mass dependence shown by (17) was used to explain the early observations of weak Ne diffraction [15]. The present analysis shows that, for Einstein oscillators, the intensity of diffraction may actually *increase* with the mass of the scattered atom. The physical reason is simply that a very heavy atom may be so slow that the Einstein oscillator is averaged out and cannot really be excited by atom scattering.

The  $C_E$  parameter appearing in (19) is a pure number giving the weight of the Einstein mode. It must be stressed that each phonon mode contributes to  $W$  according to a factor  $(\mathbf{e} \cdot \mathbf{q})^2$ , where  $\mathbf{e}$  is the polarization (unit) vector of the phonon and  $\mathbf{q}$  is the momentum transfer in the scattering process. The latter is essentially perpendicular to the surface (exactly for the specular beam, approximately for the diffracted beams), hence the relevant phonons are those polarized in the perpendicular direction:  $C_E$  measures the weight of the Einstein mode among the perpendicularly polarized phonons. Such weight is relatively large, since the Einstein mode corresponds to a frequency independent of the parallel momentum  $\mathbf{K}$  and to a purely perpendicular polarization  $\mathbf{e}$ , while the polarization of the other modes varies (roughly,  $\mathbf{e}$  is perpendicular only in one third of cases). In the  $c(2 \times 2)$  structure, these other modes involve largely repulsive interactions among adsorbed Li adatoms and we suggest that they are also unlikely to be excited by the slow Ne atoms. A similar effect is seen in He scattering from  $c(2 \times 2)\text{Na/Cu}(100)$  [33]. These additional modes would contribute a more conventional Debye–Waller effect, which usually reduces Ne diffraction considerably with respect to that of He. A further discussion of this point is given below.

Since, in the case of Li adatoms, the perpendicular vibrational frequency is known to be high,  $\nu = 9.3$  THz [34], the semiclassical theory developed above must be modified and quantum corrections are necessary. A complete quantum theory of the Debye–Waller factor for an Einstein model was presented by Kasai and Brenig [29]. Such theory is far from obvious. Here, we consider a few elementary corrections to the semiclassical theory in order to provide a more intuitive description. These corrections still capture some interesting quantum effects predicted by Kasai and Brenig, in particular the characteristic (and surprising) decrease of the elastic scattering intensity at low temperatures.

The quantum effects that we believe to be essential here are of two types. First, it must be recalled that (13) is only a classical, or high temperature, approximation to the quantum expression for  $B(\tau)$  given by (12). The latter contains a complex factor  $\exp(i\omega\tau)$  in the zero-point term. Only the real parts of the time integrals contribute, since the elastic intensity is proportional to  $|\exp(-W_G)|^2$ , and the absolute value of an exponential is the exponential of the real part. Thus, (8) can be replaced by

$$\text{Re}(W_G) = \frac{1}{2\hbar^2} \sum_{mn} \int A_{mn}(\tau) : \text{Re}(B_{mn}(\tau)) d\tau \quad (22)$$

and equation (11) by

$$\text{Re}(W) = \frac{1}{2\hbar^2} \int A(\tau) \text{Re}(B(\tau)) d\tau, \quad (23)$$

since  $A(\tau)$  (or, more generally,  $A_{mn}(\tau)$ ) is real.  $\text{Re}$  denotes the real part. Now, in the quantum expression  $\exp(i\omega\tau)$  may be replaced by  $\cos \omega\tau$ , obtaining  $\text{Re}(B(\tau))$  as

$$\text{Re}(B(\tau)) = \frac{\hbar}{M} \int \frac{g(\omega)}{\omega} \left\{ [\exp(\hbar\omega/kT) - 1]^{-1} + \frac{1}{2} \right\} \times \cos \omega\tau d\omega. \quad (24)$$

A further correction must be applied, depending on the incident energy, to account for a ‘closed channel’ effect. Indeed, the Bose–Einstein ‘ $\langle n \rangle + 1/2$ ’ term in (24) is nothing but  $\frac{1}{2}(\langle n \rangle + \langle n \rangle + 1)$ , where the terms  $\langle n \rangle$  and  $(\langle n \rangle + 1)$  are immediately recognizable as contributions from gain (absorption of quanta) and loss (emission of quanta), respectively. Focusing on the latter, for each component of the spectrum, no quanta are emitted if the incident energy  $E_z$  is less than the phonon energy,  $\hbar\omega$ , which suggests an angular dependence in reflectivity as the perpendicular energy,  $E_z = E \cos^2(\theta)$ , approaches the threshold. If  $E_z$  is larger than  $\hbar\omega$ , then emission is possible but becomes increasingly difficult as  $E_z$  approaches  $\hbar\omega$ : this can be traced to a factor  $k'_z/k_z = (1 - \hbar\omega/E_z)^{1/2}$  which arises from the phase-space available for the scattering process (corresponding to the three-dimensional density of states), and should multiply the loss term<sup>6</sup>. Hence, in order to obtain a quantum expression for  $W$ , for a general spectrum we should multiply the loss term of the integrand occurring in (24) by  $(1 - \hbar\omega/E_z)^{1/2}$  and extend the integral not to infinity, but only to  $E_z/\hbar$ . For the gain term, the same argument leads to an enhancement, rather than to a reduction, the factor being  $(1 + \hbar\omega/E_z)^{1/2}$ . Of course, the gain or absorption term is much less important at relatively low temperatures, because few quanta are present in equilibrium. For an Einstein model, there is only one frequency and the situation is more extreme. Following the same line of reasoning, the loss contribution to  $W$  would disappear whenever  $E_z < \hbar\omega_E$  and only the relatively weak Debye–Waller effect from the gain term would survive. Summarizing the above arguments and taking the ratio of the integrands in (13) and (24), we adopt a simple quantum correction factor for Einstein oscillators,  $Q(a = \hbar\omega_E/kT, b = \hbar\omega_E/E_z)$ , where

$$Q(a, b) = \begin{cases} \frac{a}{2} \left[ \frac{1}{e^a - 1} \sqrt{1+b} \right. \\ \left. + \left( \frac{1}{e^a - 1} + 1 \right) \sqrt{1-b} \right] & \text{for } b < 1 \\ \frac{a}{2} \left[ \frac{1}{e^a - 1} \sqrt{1+b} \right] & \text{for } b > 1. \end{cases} \quad (25)$$

Thus, inserting (25) into (20), we finally obtain the quantum corrected Debye–Waller term for an overlayer of Einstein oscillators. Clearly, this simple quantum correction term can also be applied in cases where the spectrum is not a delta-function. For example, in the case of a Debye spectrum, (25) should be retained inside the integral term of the classical result given by (14) and written in terms of spectral component  $\omega$  rather than the single-valued  $\omega_E$ .

The above description completes the qualitative description of Ne scattering from  $c(2 \times 2)\text{Li/Cu}(100)$  that was recently presented [24]. However, even in that paper we noted

<sup>6</sup> A simple justification for the presence of such a factor is as follows: the sum of all scattering probabilities (which is 1) may be written as the product of the Debye–Waller factor  $\exp(-2W)$  times  $\exp(2W)$ . Expanding the latter factor we get  $1 + 2W + 2W^2 + 4/3W^3 + \dots$ , where the term  $W^n$  corresponds to  $n$  quanta exchanged [28]. Thus, the exponent  $2W$  in the Debye–Waller factor for the loss term is approximately equal to the single-quantum emission probability (rather than simply proportional to it), and must contain the same kinematic factor  $k'_z$  as the latter.

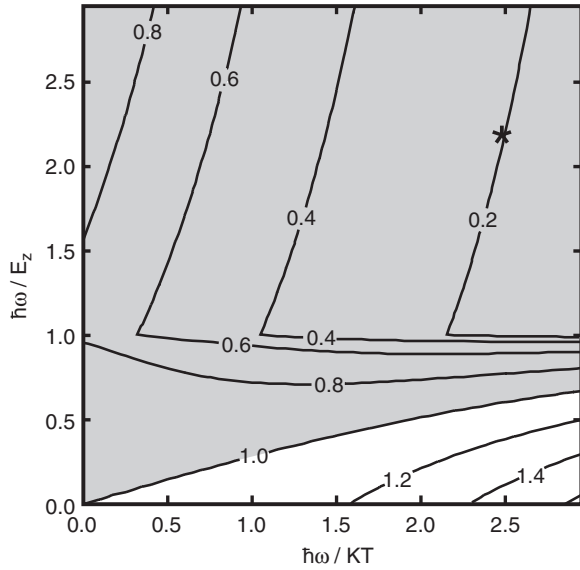


**Figure 2.** Contour plot of the quantum correction term,  $Q$ , described by (25). The region with  $Q$  less than one is shown with grey shading and corresponds to a decrease of  $W_E$  with respect to the classical result given by (20) and therefore an increase in elastic scattering. The asterisk indicates the experimental conditions of the unusually high Ne reflectivity in figure 1, predicting a 5-fold increase in specular reflectivity over the classical expectation.

the approximation to be too severe to agree quantitatively with the experimental data and we indicated that total decoupling from lower-energy substrate modes is unlikely to occur. Let us now explore an extension of the above Einstein model to account for this contribution. The Debye–Waller exponent,  $W$ , is linear in the phonon spectrum, so that if both an Einstein and a Debye spectrum (or any other spectrum) are simultaneously present then their respective contributions may simply be added. This amounts to add a contribution from the Debye part of the spectrum and it suffices to multiply the contribution by the weight  $C_D$  (with  $C_E + C_D = 1$ ). For simplicity, we extract the weighting factor from (19) and add the Einstein and Debye contributions as:

$$W = C_E W_E + (1 - C_E) W_D. \quad (26)$$

The Einstein overlayer contribution is given by (20) and (25) and the Debye contribution is given by (17), (18) and (25), remembering that whilst  $\omega_E$  denotes a single vibrational term,  $\omega_D$  scales an entire spectrum. The Debye term has previously been shown to vary with  $\sqrt{m}$ . The Einstein term, on the other hand, is the product of an  $m^2$  dependence and hyperbolic functions that tend, for large arguments, to  $\exp(-c\sqrt{m})$  (where, for simplicity, other variables have been collected together in a single term,  $c$ ). Thus, the mass dependence of (26) can become rather complex, depending on the precise values of  $C_E$  and the atom–surface potential parameters  $\alpha$  and  $\epsilon$ .

### 5. Comparison between theory and experiments

We will now apply the theory developed in section 4 to the experimental data, considering only those experimental conditions where the effects of diffuse elastic scattering from

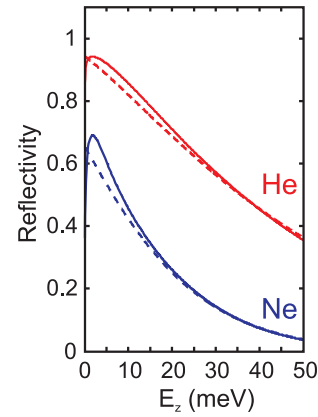


**Figure 3.** Calculated variation in reflectivity for He (red) and Ne (blue) scattering from Cu(100) using classical (dashed lines) and quantum corrected (full lines) forms of (17), as discussed in the text. Since a Debye spectrum is assumed and includes components at all energies up to  $\hbar\omega_D$ , the difference between the two curves is small and the quantum correction only has a noticeable effect at very low beam energies, where the number of accessible phonons becomes restricted.

aperiodic adatoms and defects can be neglected: the clean Cu(100) surface and the  $c(2 \times 2)$  Li overlayer at a coverage of 0.5 ML. In general, we should first consider the quantum correction term of (25), the variation of which is plotted in figure 2 for the Ne–Li system. The shaded region shows  $Q < 1.0$ , which indicates a reduction in  $W_E$  and hence a quantum enhancement over the classical result, (20) and indicates the importance of  $Q$  at low energies. The closed channel effect gives rise to a gradient discontinuity running horizontally along the line  $\hbar\omega/E_z = 1$  and splits the quantum correction into two regimes. The asterisk in figure 2 indicates the regime in which the experimental data of section 2 were collected, where the scattered atom has insufficient energy to excite an Einstein phonon mode, increasing reflectivity. More interesting behaviour is observed, however, for  $\hbar\omega/E_z < 1$ , where the scattered atom can donate energy to the surface and where this loss term rapidly dominates  $W_E$ . Note in particular the result that for much of this regime, an increase in  $\hbar\omega/kT$  (i.e. a decrease in surface temperature) now *increases*  $W_E$ , a rather counter-intuitive result that can be related to a similar effect found previously by Kasai and Brenig [29].

We may also consider the effect of  $Q$  on the scattering of He and Ne from the clean Cu(100) substrate, where (25) should be applied to each component in the Debye vibrational spectrum. The effect is illustrated in figure 3, which plots the reflectivity of He and Ne at a Cu(100) surface, both with (full lines) and without (dashed lines) the quantum correction. The curves of figure 3 were calculated numerically by incorporating the appropriate form of  $Q$  inside the integral of (14), and using 270 K ( $\hbar\omega_D = 23.3$  meV) for the Cu(100) surface Debye temperature [35]. The scattering conditions were those of figure 1. Appropriate values for the atom–surface interaction potential were obtained by fitting a Morse function to potentials described in the literature. We used experimental sources rather than *ab initio* calculations [21] since the latter do not provide a good description of the van der Waals

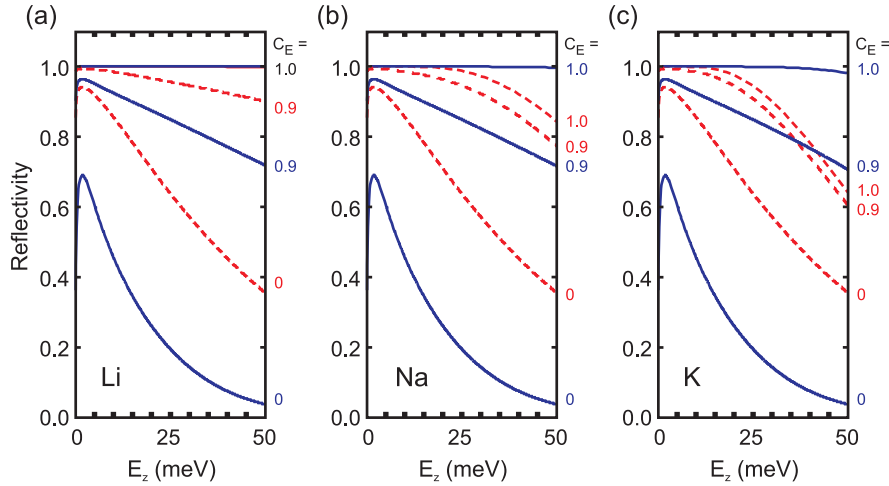


**Figure 4.** Calculated variation in reflectivity for He and Ne scattering from (a)  $c(2 \times 2)$ Li-Cu(100), (b)  $c(2 \times 2)$ Na-Cu(100) and (c) K-Cu(100) as a function of perpendicular energy  $E_z$  and for three Einstein weighting factors  $C_E$ , (0, 0.9 and 1.0, as indicated to the right of each panel). He curves are presented as red dashed lines whilst Ne curves are full blue lines.  $W_D$  was calculated numerically using (17), (18) and (25) whilst  $W_E$  was calculated using (20) and (25), using the fitted potential parameters of table 1 and  $\hbar\omega_E(\text{Li}) = 38.0$  meV;  $\hbar\omega_E(\text{Na}) = 18.5$  meV and  $\hbar\omega_E(\text{K}) = 13$  meV. See text for details.

interaction. Our fitted parameters are similar to those used elsewhere [23, 36] and are given in table 1. This calculation of  $W$  neglects some more subtle effects [30, 35, 36] but is sufficient to demonstrate the effect of the quantum correction. It is clear that the quantum correction is only significant for energies below approximately 30 meV for He and 20 meV for Ne and note in particular that since we plot reflectivity, given by  $\exp(-2W_D)$ , the differences in  $W_D$  are rather small. For most of the low-energy range the quantum correction enhances the reflectivity, similar to the trends evident in figure 2, but the enhancement is relatively small, being approximately 13% at its maximum for neon and approximately 4% maximum for helium. Since there is a full spectrum of phonon energies present, it is only at very low beam energies that the number of accessible phonons becomes restricted. Otherwise, and as might be expected, there is a strong variation in reflectivity with  $E_z$ , with the surfaces all being more reflective for He than for Ne. As  $E_z$  tends to zero, the calculated reflectivity does not tend to one because a Ne (or He) atom, even if it had no kinetic energy at long distances, accelerates in the potential well and therefore is still able to exchange energy with the surface.

In reality, the  $Q(\frac{\hbar\omega_E}{kT}, \frac{\hbar\omega_E}{E_z})$  term does not dominate the experimental results for Ne scattering from  $c(2 \times 2)$ Li-Cu(100). On one hand, the arguments of the hyperbolic terms of the Einstein contribution (20) are already sufficiently large that  $W_E$  is essentially negligible. This contribution would be relatively more important for systems where the Einstein frequency is less extreme. On the other hand, even if substantial coupling to the substrate Cu(100) modes is possible, the effect of the quantum correction on  $W_D$  is weak, as shown by figure 3. As a consequence, the impact of (26) is to provide a linear variation of  $W$  with  $C_E$ , ranging from the clean Cu(100) value ( $C_E = 0$ ) to effectively zero ( $C_E = 1$ ), where complete quantum scattering occurs. This strong dependence on  $C_E$  allows an unambiguous fit to the data and we find that in order to achieve the high reflectivities observed,

**Table 1.** Fitted Morse potential parameters for He and Ne scattering from Cu(100), Li, Na and K, using the data provided in [36, 39].

		Cu(100)	Li	Na	K
He	$\alpha$ ( $\text{\AA}^{-1}$ )	1.01	0.84	0.79	0.71
	$\epsilon$ (meV)	5.63	1.54	1.08	0.70
Ne	$\alpha$ ( $\text{\AA}^{-1}$ )	1.07	0.84	0.77	0.66
	$\epsilon$ (meV)	11.67	4.34	3.20	2.23

$C_E$  must be 0.9 or greater. The effect of  $C_E$  is explored further in figure 4, which plots the He and Ne reflectivity of  $c(2 \times 2)$ Li-Cu(100) as a function of perpendicular energy,  $E_z$ , for three  $C_E$  values (0, 0.9 and 1.0, indicated to the right of the plot). Also plotted are the expected results for Na and K overlayers. The Na overlayer is known to adopt a  $c(2 \times 2)$  structure [33] whilst K adopts a quasi-hexagonal hexagonal structure [37] and may therefore behave similarly in Debye-Waller terms, the principal differences with respect to the Li system being changes to the interaction potential and to the Einstein frequencies,  $\omega_E$ . The Einstein frequencies for Na and K were taken as 18.5 meV and 13.0 meV, respectively [38], whilst the same details were used for the Cu(100) surface as outlined above. In order to calculate the data of figure 4 we obtained values for the atom-surface interaction by fitting a Morse function to the data of [39] and the fitted parameters are again presented in table 1. Note that, by using gas-phase interaction potentials for the alkali metals, we are effectively neglecting any adsorbate polarization upon adsorption, and thereby neglecting any resulting increase of  $\epsilon$  [21]. Note also that the calculated trends neglect any additional causes for a reduction in specular intensity, particularly variations in diffuse scattering cross-section and elastic scattering into diffraction channels, which we can expect to occur for Ne scattering from all three systems [24].

First, let us note that the calculated trends for  $C_E = 0$  in figure 4, which correspond to the expectation for the clean



Cu(100) surface, are identical to those of figure 3. At the other extreme, setting  $C_E = 1$  has a dramatic effect in all cases. For the Li system,  $C_E = 1$  leads to a reflectivity that is independent of  $E_z$  in the range studied (both curves overlap at reflectivity = 1). This invariance is a direct consequence of the high vibrational frequency of Li and of the inability of Ne or He to exchange energy with the Einstein oscillations. Very similar trends are calculated for both Na or K adsorbates, despite reductions in  $\omega_E$ , suggesting that experimental data from these systems would be worth collecting. In each case, note that the Ne curve now lies *above* the curve for He, a consequence of the slower Ne atom as it crosses the atom–surface potential well. The increase is accordance with the discussion of the unusual  $m$  dependence of  $W$  in section 4. The importance of this result now depends critically on the value of  $C_E$ , which we believe to be close to 0.9 for the experimental situation for Li. In this case, the calculations indicate a rather modest variation in reflectivity with  $E_z$  for both He and Ne scattering from Li. The He reflectivity is predicted to be higher than that of Ne, but the difference is rather small and agreement with experiment is therefore excellent. Turning to the calculations for Na, the difference between He and Ne reflectivities is more substantial. At  $C_E = 0.9$ , attenuation due to substrate phonons still dominates and the He reflectivity remains higher than Ne reflectivity. Clearly, however, a slight decrease in  $C_E$  could reverse that situation. Indeed, in the absence of other effects, taking  $C_E = 0.9$  for the K overlayer results in Ne reflectivity exceeding He reflectivity for  $E_z > 40$  meV. Such an observation has never been made experimentally but would be a remarkable display of the counter-intuitive consequences of the theory developed in this paper.

## 6. Discussion

In recent years it has become increasingly clear that a number of physical phenomena, which usually appear to behave in a completely classical fashion, do so only because of decoherence and are ready to show quantum features as soon as the causes of decoherence are in abeyance. In the case of atom–surface scattering the main cause of decoherence is phonon emission (and absorption), which, via a strong Debye–Waller effect, tends to destroy quantum scattering (i.e. diffraction) for all but the lightest atoms. Elastic, quantum scattering was detected many years ago with Ne atoms [1, 2] and more recently an elastic component has been detected with heavier noble gases [6–8, 12, 20], especially in cases where phonon exchange was weak, either because of low temperature, or because of grazing incidence of the atom beam. The discussion outlined above shows a more striking effect: for an ordered adsorbate of Li on Cu the relevant phonons have such a high frequency that phonon exchange disappears, with the result that at the coverage where the ordered  $c(2 \times 2)$  adsorbate forms, the diffraction of the slow Ne atoms is as strong as He diffraction. We have shown that this surprising observation is, in fact, in agreement with theory. Equations (20) and (25) show that, for an Einstein model, the increase of the Debye–Waller exponent  $W$  due to the  $m^2$  factor can be more than compensated by the exponential decrease related to the

hyperbolic functions. Physically, this reflects the fact that the Einstein mode, corresponding to the high frequency  $\omega_E$ , is averaged out and cannot be effectively excited during the slow scattering process. Another way of expressing this is to say that the surface scattering is largely adiabatic. Thus, if low frequency modes are absent or unimportant,  $W$  remains small and the scattering remains quantum mechanical and elastic. This appears to be precisely the case for the  $c(2 \times 2)$ Li/Cu(100) adsorbate, where low-energy T-mode phonons are weak: a quasi-Einstein mode survives, but the probability of energy exchange with a scattered Ne atom is small.

The theory described in section 4, being based on a pure Einstein model, is necessarily approximate. If taken literally, it would lead to a paradoxical result that above a certain atom mass  $W$  would decrease and the scattering would become increasingly quantum mechanical and elastic as the atom mass increases (and correspondingly, the scattering time gets longer). Such a paradox would not occur in practice because the spectrum is never purely Einstein-like and the contribution of low frequency modes, however small, will always cause the scattering of heavy atoms to be more inelastic as the mass increases. To analyse this point, we have discussed the effect of adding a Debye part to the phonon spectrum, showing that, although the main points of the present theory hold, the paradoxes are thereby eliminated. An accurate comparison with experiments in section 2 is based, indeed, on such assumption of a phonon spectrum comprising both an Einstein and a Debye contribution.

## Acknowledgments

We are thankful to Piero Calvini and Riccardo Ferrando for critical reading of the manuscript.

## References

- [1] Boato G, Cantini P, Garibaldi U, Levi A C, Mattera L, Spadacini R and Tommei G E 1973 *J. Phys. C: Solid State Phys.* **6** L394
- [2] Boato G, Cantini P and Mattera L 1976 *Surf. Sci.* **55** 141
- [3] Rieder K H and Stocker W 1985 *Phys. Rev. B* **31** 3392
- [4] Parschau G, Kirsten E, Bischof A and Rieder K H 1989 *Phys. Rev. B* **40** 6012
- [5] Salanon B 1984 *J. Physique* **45** 1373
- [6] Althoff F, Andersson T and Andersson F 1997 *Phys. Rev. Lett.* **79** 4429
- [7] Althoff F, Andersson T and Andersson F 1998 *Phys. Rev. Lett.* **81** 1743
- [8] Schweizer E K and Rettner C T 1989 *Phys. Rev. Lett.* **62** 3085
- [9] Schüller A, Wethekam S and Winter H 2007 *Phys. Rev. Lett.* **98** 016103
- [10] Rousseau P, Khemliche H, Borisov A G and Roncin P 2007 *Phys. Rev. Lett.* **98** 016104
- [11] Farias D and Rieder K-H 1998 *Rep. Prog. Phys.* **61** 1575 and references therein
- [12] Berenbak B, Zboray S, Riedmüller B, Papageorgopoulos D C, Stolte S and Kleyn A W 2002 *Phys. Chem. Chem. Phys.* **4** 68
- [13] Hayes W W and Manson J R 2007 *Phys. Rev. B* **75** 113408
- [14] Böheim J and Brenig W 1981 *Z. Phys. B* **41** 243
- [15] Levi A C and Suhl H 1979 *Surf. Sci.* **88** 221
- [16] Burke K and Kohn W 1991 *Phys. Rev. B* **43** 2477
- [17] Gumhalter B 1996 *Surf. Sci.* **347** 237

- [18] Šiber A and Gumhalter B 1997 *Surf. Sci.* **385** 270
- [19] Šiber A and Gumhalter B 1998 *Phys. Rev. Lett.* **81** 1742
- [20] Andersson T, Althoff F, Linde P, Andersson S and Burke K 2002 *Phys. Rev. B* **65** 045409
- [21] Brivio G P and Trioni M I 1999 *Rev. Mod. Phys.* **71** 231
- [22] Trioni M I, Marcotulio S, Santoro G, Bortolani V, Palumbo G and Brivio G P 1998 *Phys. Rev. B* **58** 11043
- [23] Pollak E, Sengupta S and Miret-Artés S 2008 *J. Chem. Phys.* **129** 054107
- [24] MacLaren D A, Huang C, Levi A C and Allison W 2008 *J. Chem. Phys.* **129** 094706
- [25] Lapujoulade J, Lejay Y and Armand G 1980 *Surf. Sci.* **95** 107
- [26] van Hove L 1954 *Phys. Rev.* **95** 249
- [27] Garibaldi U, Levi A C, Spadacini R and Tommei G E 1975 *Surf. Sci.* **48** 649
- [28] Glauber R J 1955 *Phys. Rev.* **98** 1692
- [29] Kasai H and Brenig W 1985 *Z. Phys. B* **59** 429
- [30] Gumhalter B 2001 *Phys. Rep.* **351** 1
- [31] Braun J, Fuhrmann D, Bertino M, Graham A P, Toennies J P, Wöll Ch, Bilić A and Gumhalter B 1997 *J. Chem. Phys.* **106** 9922
- [32] Manson J R, Graham A P and Li M 2002 *J. Phys.: Condens. Matter* **14** 6233
- [33] Graham A P and Toennies J P 1997 *Phys. Rev. B* **56** 15378
- [34] Tero R, Sasaki T and Iwasawa Y 2000 *Surf. Sci.* **448** 250
- [35] Hofmann F, Toennies J P and Manson J R 1994 *J. Chem. Phys.* **101** 10155
- [36] Jackson B 1990 *J. Chem. Phys.* **92** 1458
- [37] Diehl R and McGrath R 1996 *Surf. Sci. Rep.* **23** 43
- [38] Astaldi C, Rudolf P and Modesti S 1990 *Solid State Commun.* **75** 847
- [39] Chizmeshya A, Cole M W and Zaremba E 1998 *J. Low Temp. Phys.* **110** 677